

# **PROGRESS PRESENTATION 2**

## **Quantum Optimization in Location Tracking Systems**

**Team: Conqueror**

**By: Mohamed Khalil Brik**

***Supervised By: Dr Moustafa Youssef***



# OVERVIEW

**1. Introduction**

**2. Background**

**3. Problem Statement**

**4. Architecture**

**5. QUBO Formulation**

**6. Results**

**7. Research Paper**

**8. Future Work**

**Appendix**

# 1. Introduction

## INDOOR LOCALIZATION: KEY USES



INCIDENT MANAGEMENT



EMERGENCY RESPONSE



RETAIL BEHAVIOR  
INSIGHTS



INDUSTRIAL AUTOMATION  
& LOGISTICS

## WiFi Fingerprinting



Fingerprinting performance depends on:



Access Point  
(AP) quality



AP placement & density



AP selection strategy

These directly impact:

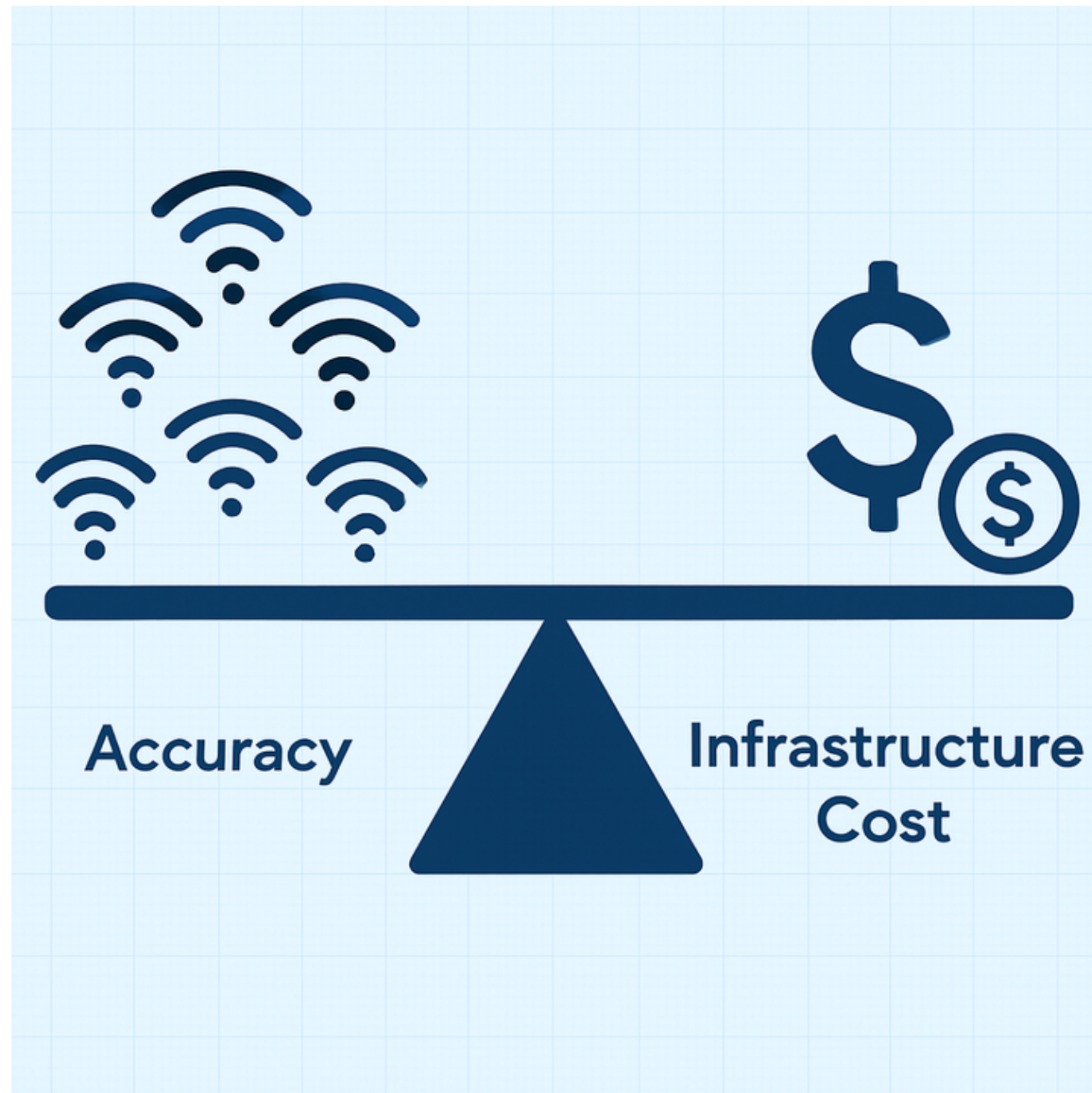


Localization accuracy



Computational cost

# 1. Introduction



**Solution →**  
**Quantum annealing for AP selection with budget constraints**

## **2. Background**

**2.1 3D FINGERPRINTING**

**2.2 QUANTUM ANNEALING**

# 2.1 3D Fingerprinting

## 1. Offline Calibration Phase:

- Collects RSS measurements from all visible APs at known reference points throughout the 3D space
- Fingerprint =  $\{(x, y, z), [RSS_1, RSS_2, \dots, RSS_n]\}$
- Creates radio map database linking locations to signal patterns

## 2. Online Localization Phase:

- User's device measures RSS values from nearby APs and matches against the pre-built database
- Match → Estimated Position  $(\hat{x}, \hat{y}, \hat{z})$
- Uses k-NN or other algorithms to find best matching fingerprint

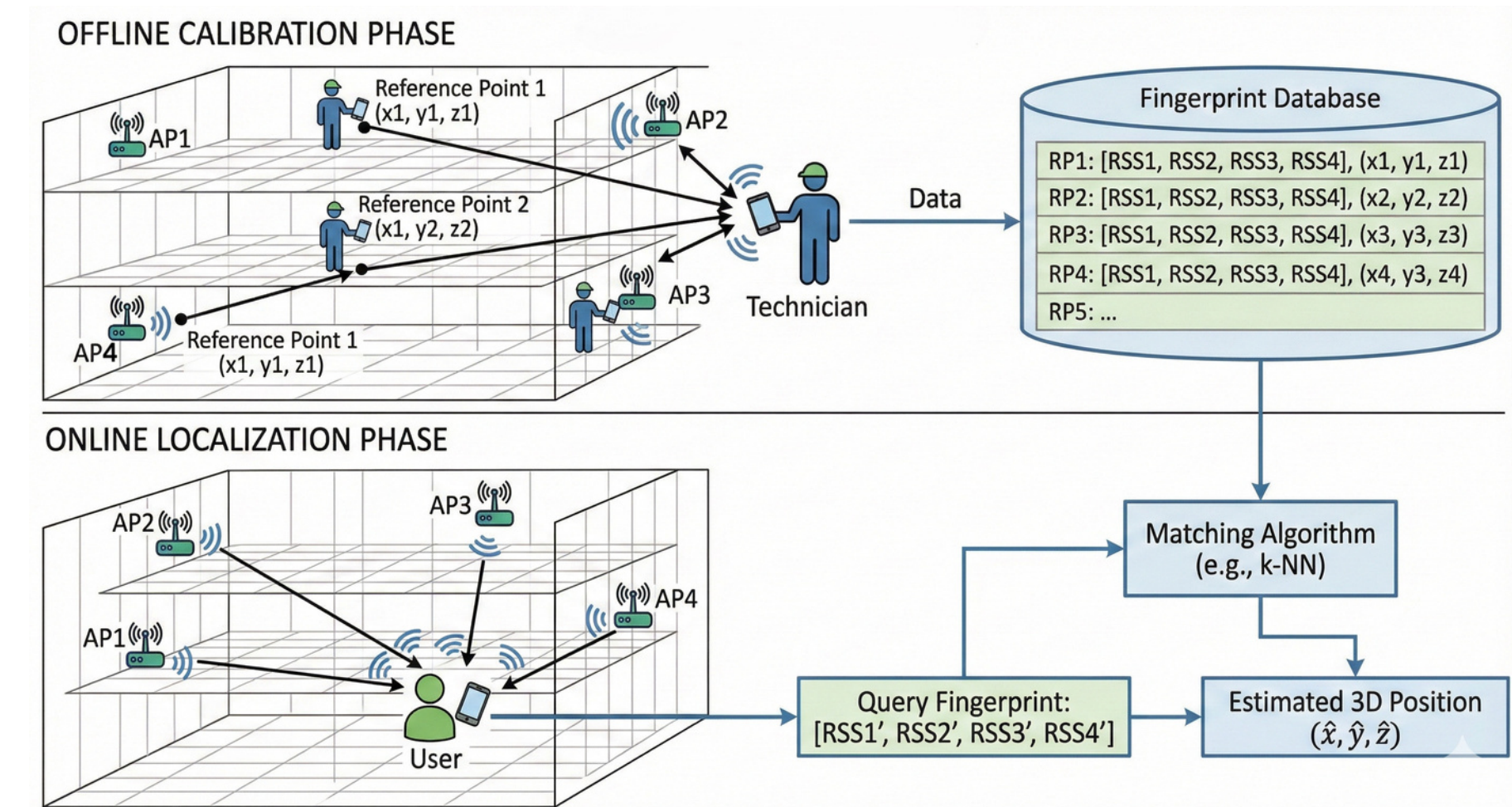


Fig. 1: Example of WiFi fingerprinting location tracking process with four APs.

# 2.2 Quantum Annealing

## 1. Problem Encoding:

- Convert optimization problem into QUBO form
- Define objective function  $Q(x)$  with binary variables
- Map to Ising Hamiltonian  $H_f$  (target Hamiltonian)

## 2. Initialization:

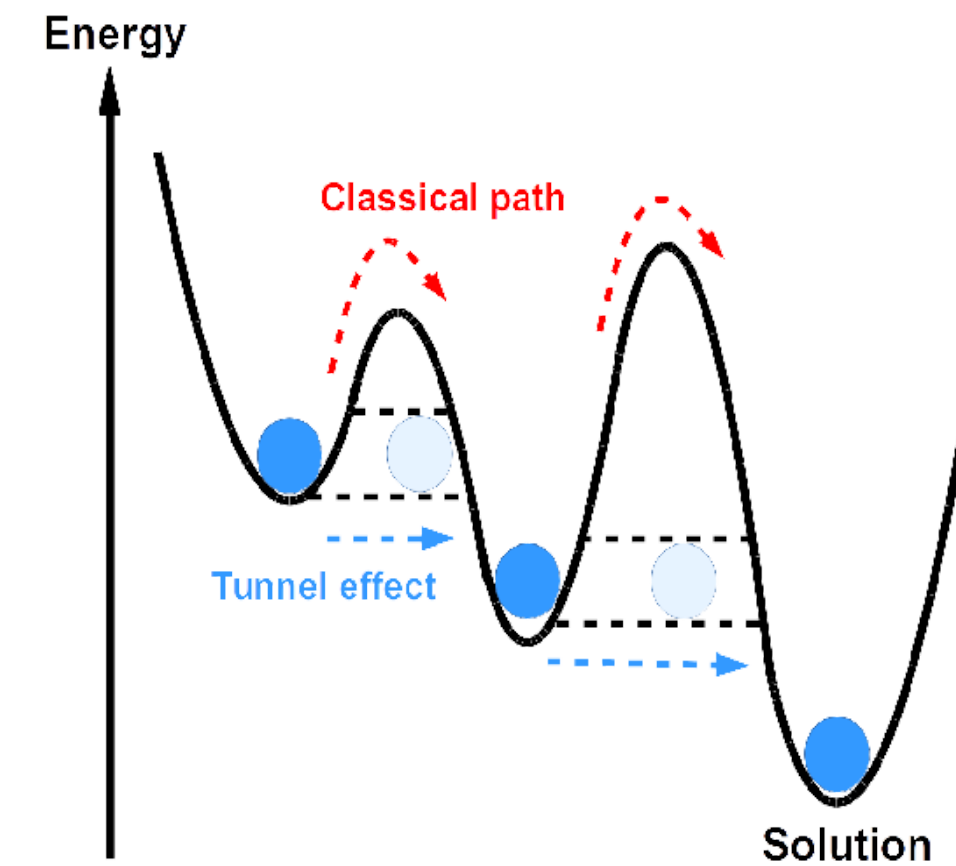
- System starts in ground state of simple Hamiltonian  $H_0$

## 3. Adiabatic Evolution:

- System slowly evolves from  $H_0$  to  $H_f$
- Governed by:  $H(t) = (1 - s(t))H_0 + s(t)H_f$
- $s(t)$  varies from 0 to 1 over annealing time

## 4. Measurement:

- Final state encodes optimal solution (binary)



Quantum Tunnelling

Fig. 2: Quantum Tunneling

### 3. Problem Statement

How can we select  $n$  APs  
from  $k$  candidates to  
maximize accuracy in a 3D  
Environment?



# 4. Architecture

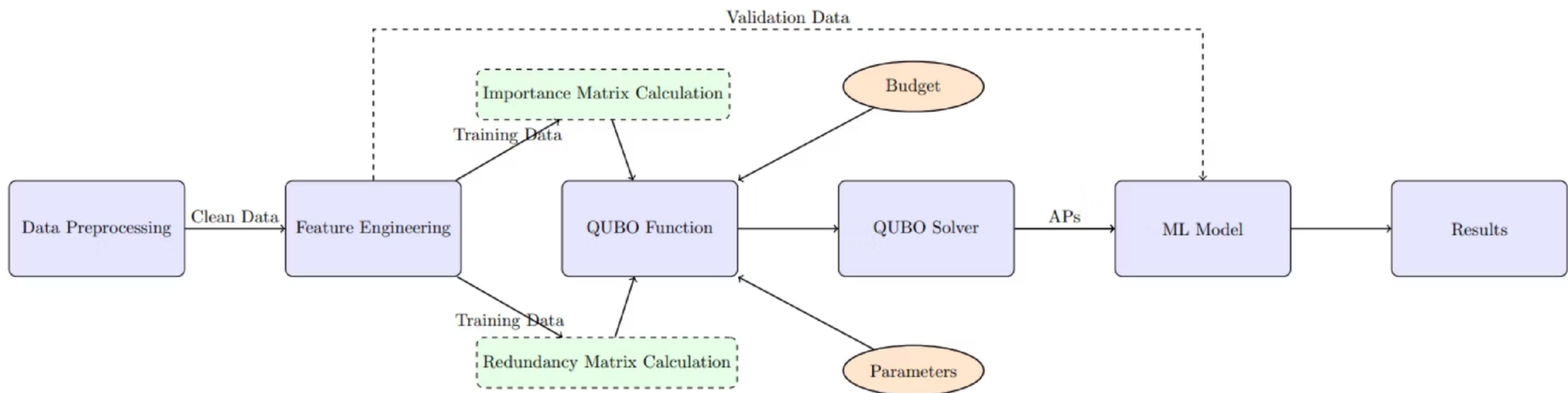


Fig. 3: System Architecture.

# 5. QUBO Formulation

$$Q(\mathbf{x}, \alpha) = -\alpha \sum_{i=1}^n I_i x_i + (1 - \alpha) \sum_{i=1}^n \sum_{j>i} R_{ij} x_i x_j + \eta \left( \sum_{i=1}^n x_i - k \right)^2$$

TABLE I: Table of Notations

Symbol	Description
$Q(\mathbf{x}, \alpha, \eta)$	The QUBO objective function.
$\mathbf{x}$	A binary AP selection vector of size $n$ .
$x_i \in \mathbf{x}$	$x_i = 1$ if AP $i$ is selected, 0 otherwise.
$\alpha$	The balancing parameter ( $0 \leq \alpha \leq 1$ ).
$n$	The total number of candidate APs.
$m$	The total number of samples in the fingerprint.
$k$	The desired number of APs to select.
$\eta$	The penalty coefficient for the constraint.
$I_i$	The calculated importance score for AP $i$ .
$R_{ij}$	The redundancy score between APs $i$ and $j$ .
$r_i, r_j$	Vectors of RSS measurements for APs $i$ and $j$
$r_{i,l}$	The $l$ -th RSS measurement for AP $i$ .
$\bar{r}_i$	The mean of the RSS vector for AP $i$ .

# **6. Results**

**6.1 Importance metrics**

**6.2 Entropy Importance**

**6.3 Redundancy**

**6.4 Alpha Parameter Impact**

**6.5 Budget (k) Impact**

**6.6 Penalty Impact**

**6.7 Inverse Temperature Impact**

**6.8 QA VS SA**

# 6.1 Importance Metrics

$$I_i^{\text{ENT}} = - \sum_{l \in m} p(r_{i,l}) \log_2 p(r_{i,l})$$

$$I_i^{\text{VAR}} = \frac{1}{m-1} \sum_{l=1}^m (r_{i,l} - \bar{r}_i)^2$$

$$I_i^{\text{AVG}} = \bar{r}_i = \frac{1}{m} \sum_{l=1}^m r_{i,l}$$

$$I_i^{\text{MAX}} = \max_{l=1,\dots,m} r_{i,l}$$

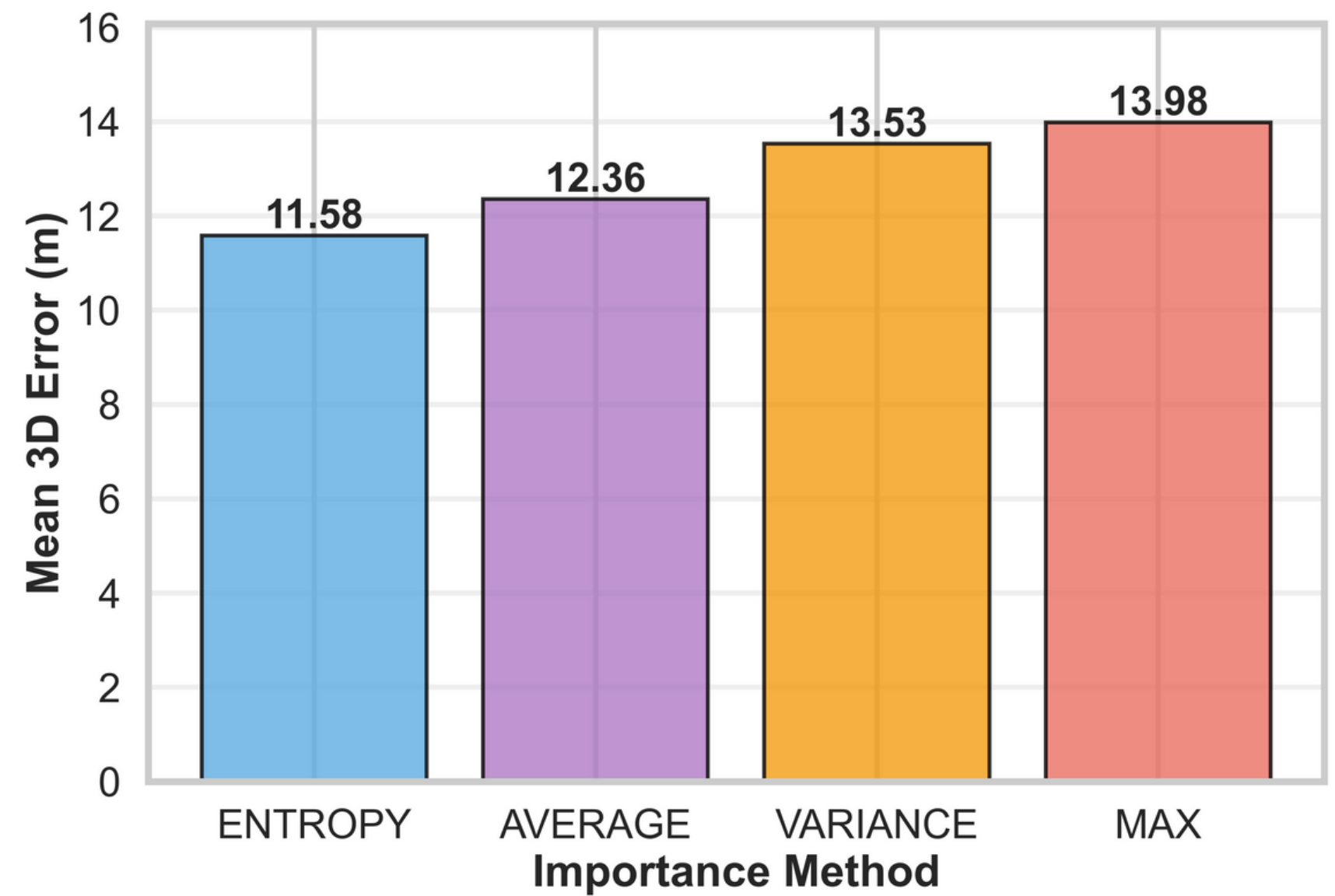


Fig. 4: Importance Methods Comparison.

## 6.2 Entropy Importance

- Many APs have zero importance.
- Zero Importance → Not Relevant APs
- We only choose APs with non-zero Importance
- The higher AP Importance value → The more relevant the AP

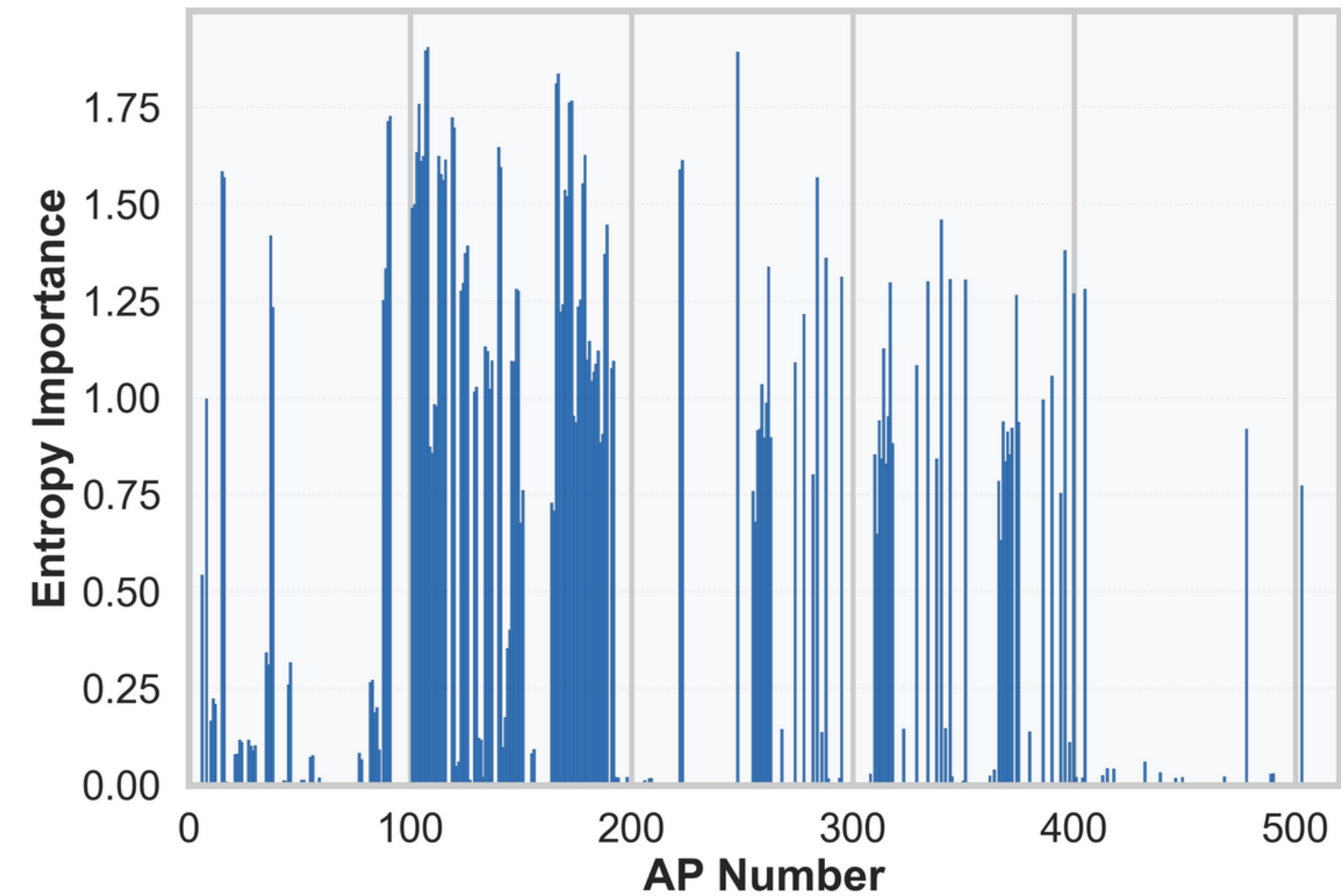


Fig. 5: Entropy Importance.

# 6.3 Redundancy

- We use only the non-zero importance APs
- We calculate the Absolute Pearson Correlation
- Highly correlated APs tell the same information
- We chose APs that are least correlated to diversify our set of APs

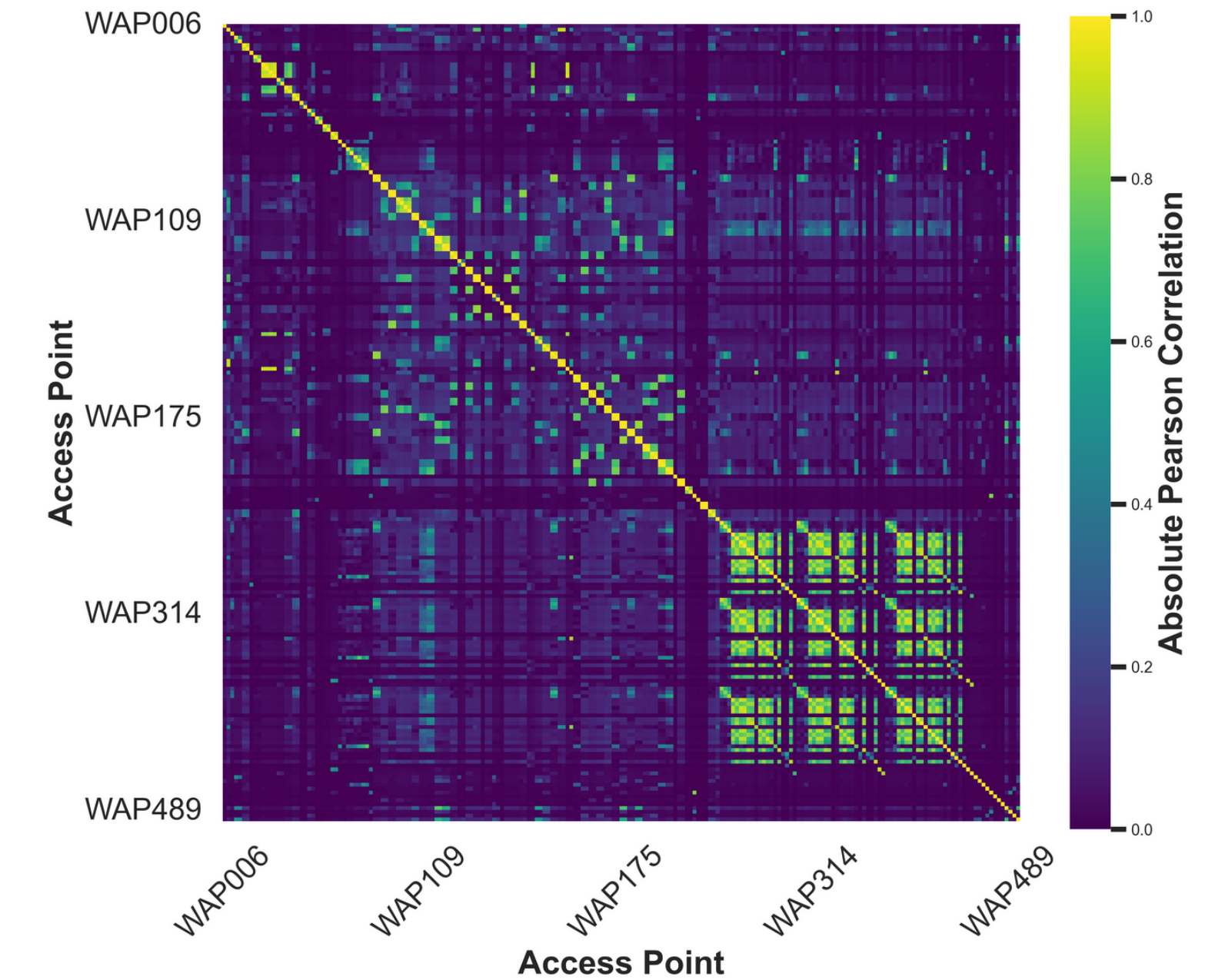


Fig. 6: Pairwise correlation matrix of AP RSS patterns.

# 6.4 Alpha Parameter Impact

- We test multiple values of alpha.
- We record the Localization Error for each.
- Best Alpha = 0.8
- Balances Importance and Redundancy

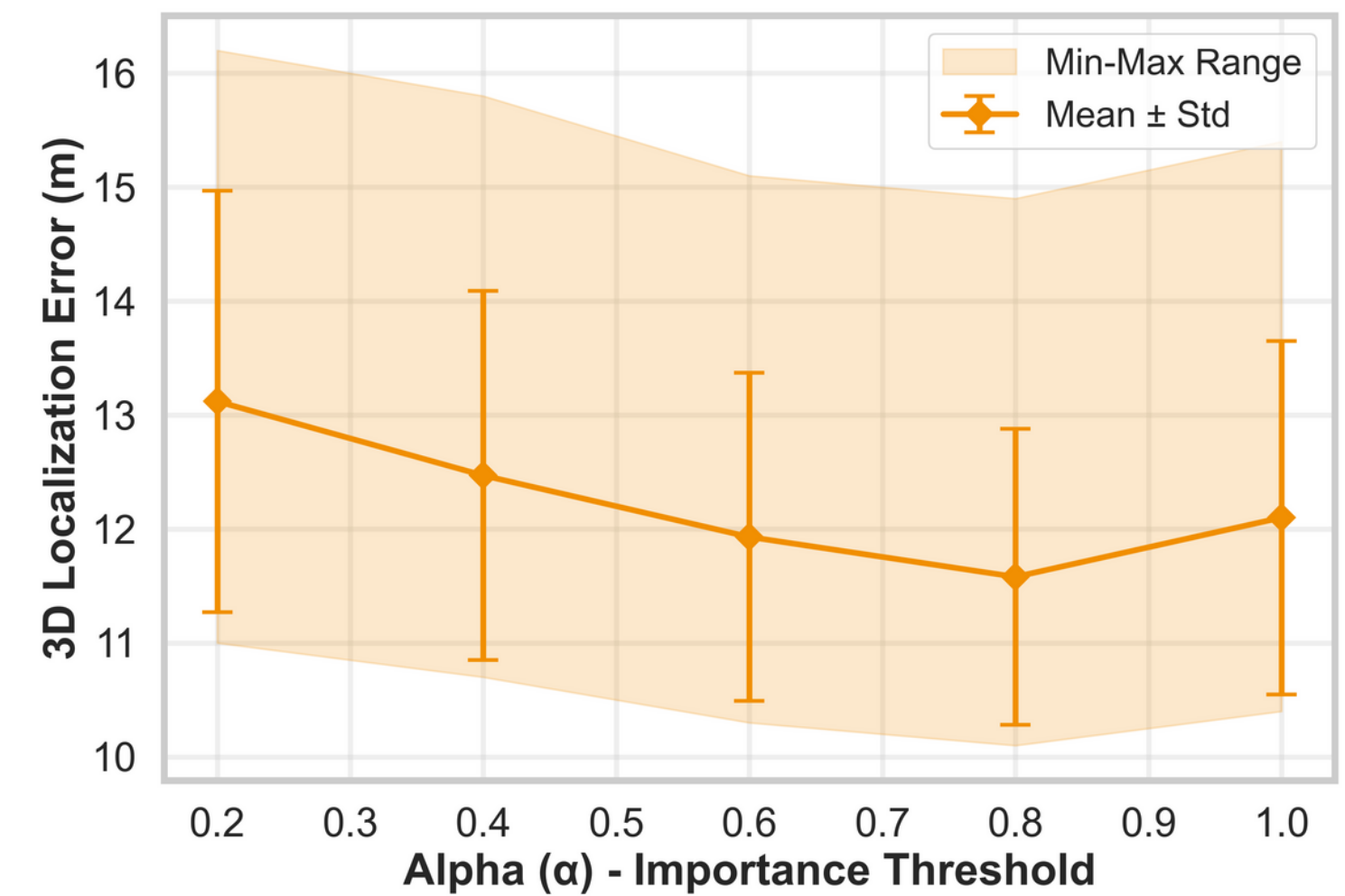


Fig. 7: Impact of Alpha on the 3D Localization Error.

# 6.5 Budget ( $k$ ) Impact

- We try different values for the budget ( $k$ )
- Run the full system.
- We can see how the budget choice impacts Accuracy.
- Generally, the higher the AP count, the lower the accuracy.

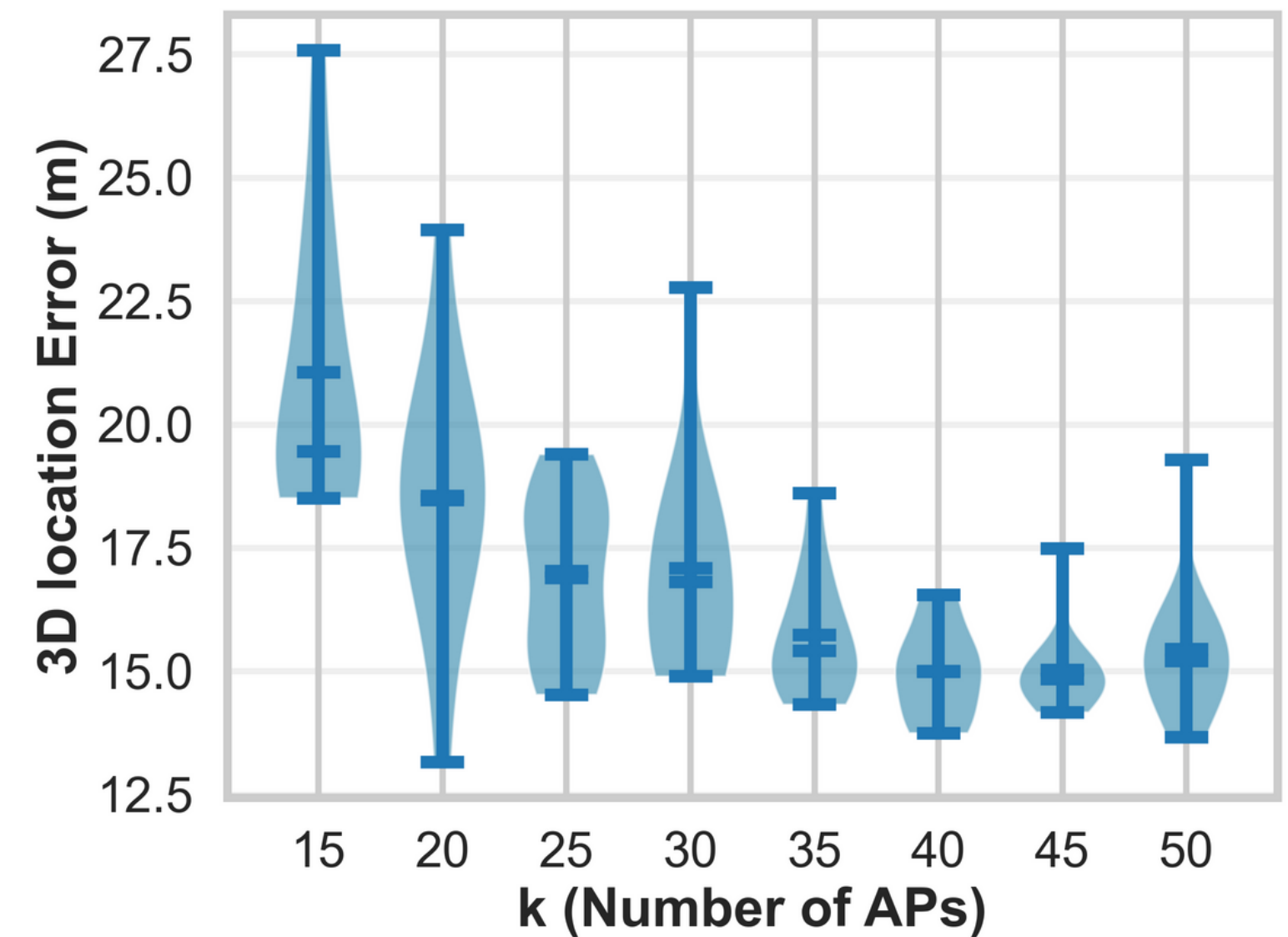


Fig. 8: Impact of  $k$  on 3D Localization Accuracy.

# 6.6 Penalty Impact

- For small values of the penalty: the optimiser can reach the target of k APs with a minimum localisation accuracy at  $\eta = 2$ .
- For larger penalty values, the constraint term creates an overly harsh energy landscape, causing the annealer to get trapped in local minima before reaching the target number of APs k, which in turn affects the localization accuracy.

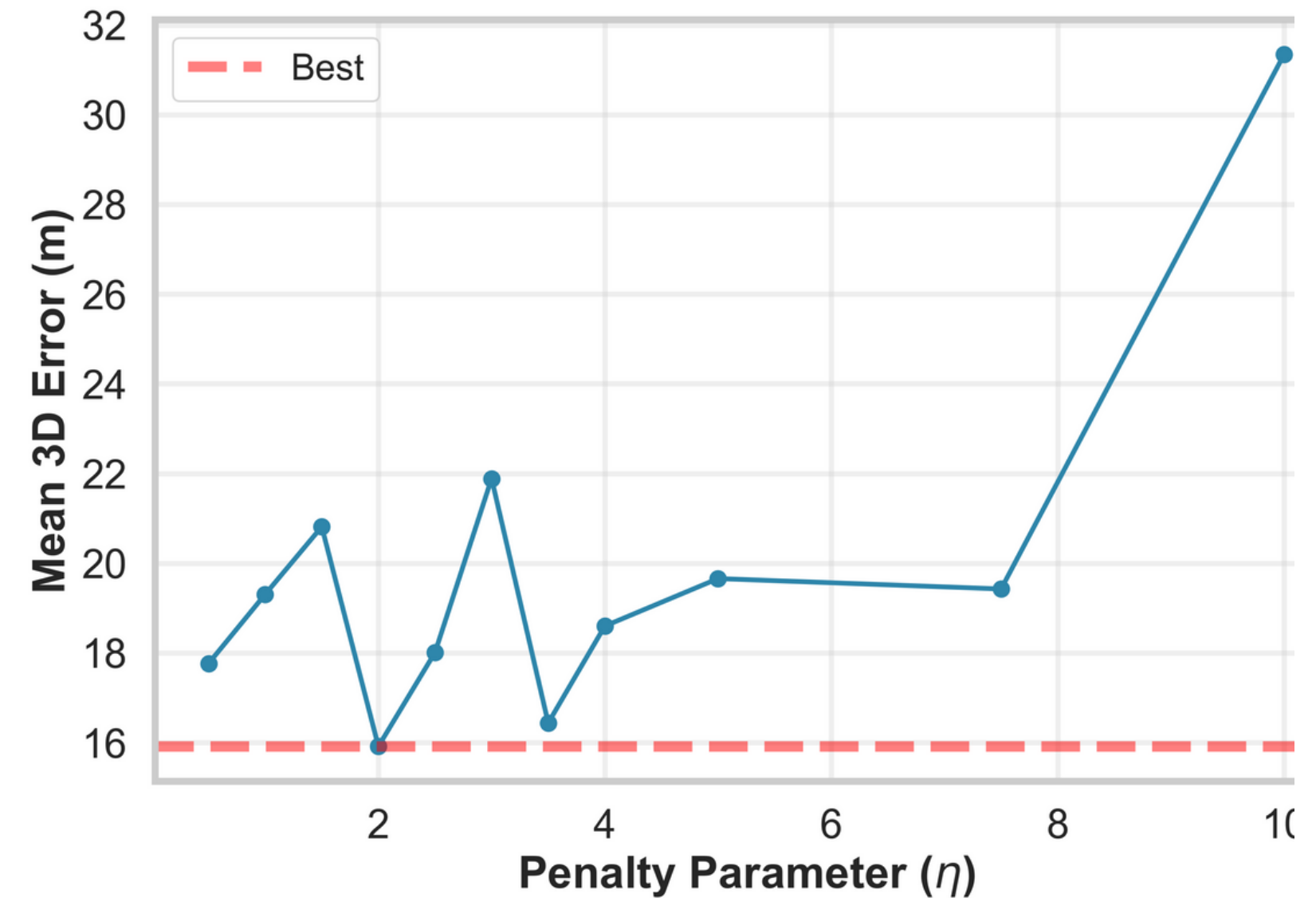


Fig. 9: Pairwise correlation matrix of AP RSS patterns.

# 6.7 Inverse Temperature Impact

- $\beta$  functions as a scaling factor that controls the influence of the problem's energy landscape.
- $\beta$  determines how sharply the solver distinguishes between optimal and suboptimal solutions.
- Localization accuracy improves as  $\beta$  increases.
- Improvement stops at  $\beta = 5$

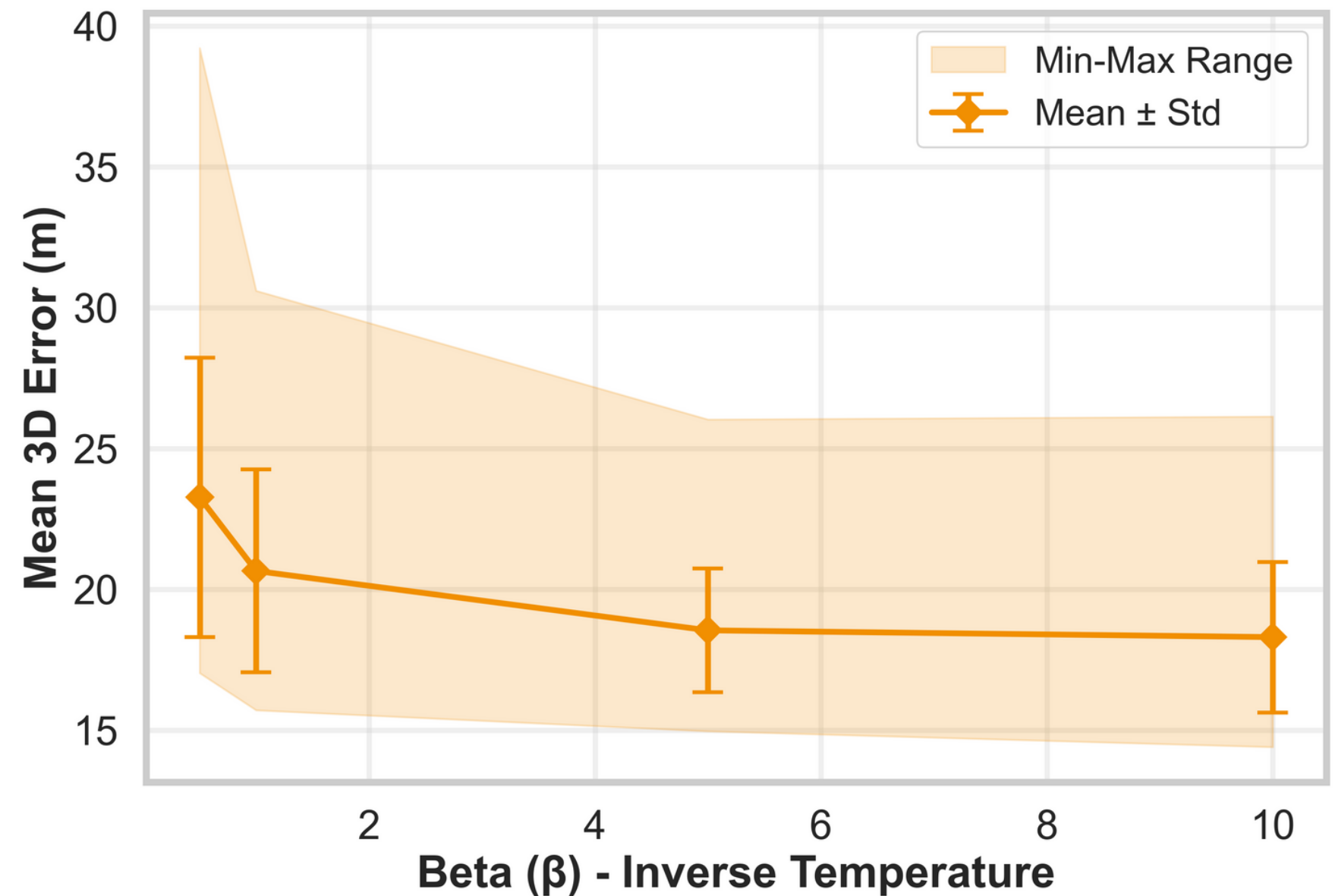


Fig. 10: Impact of  $\beta$  on the Mean 3D Localization Error.

# 6.8 QA VS SA

- QA has the best exact floor accuracy localization
- Better than using the entire set of APs

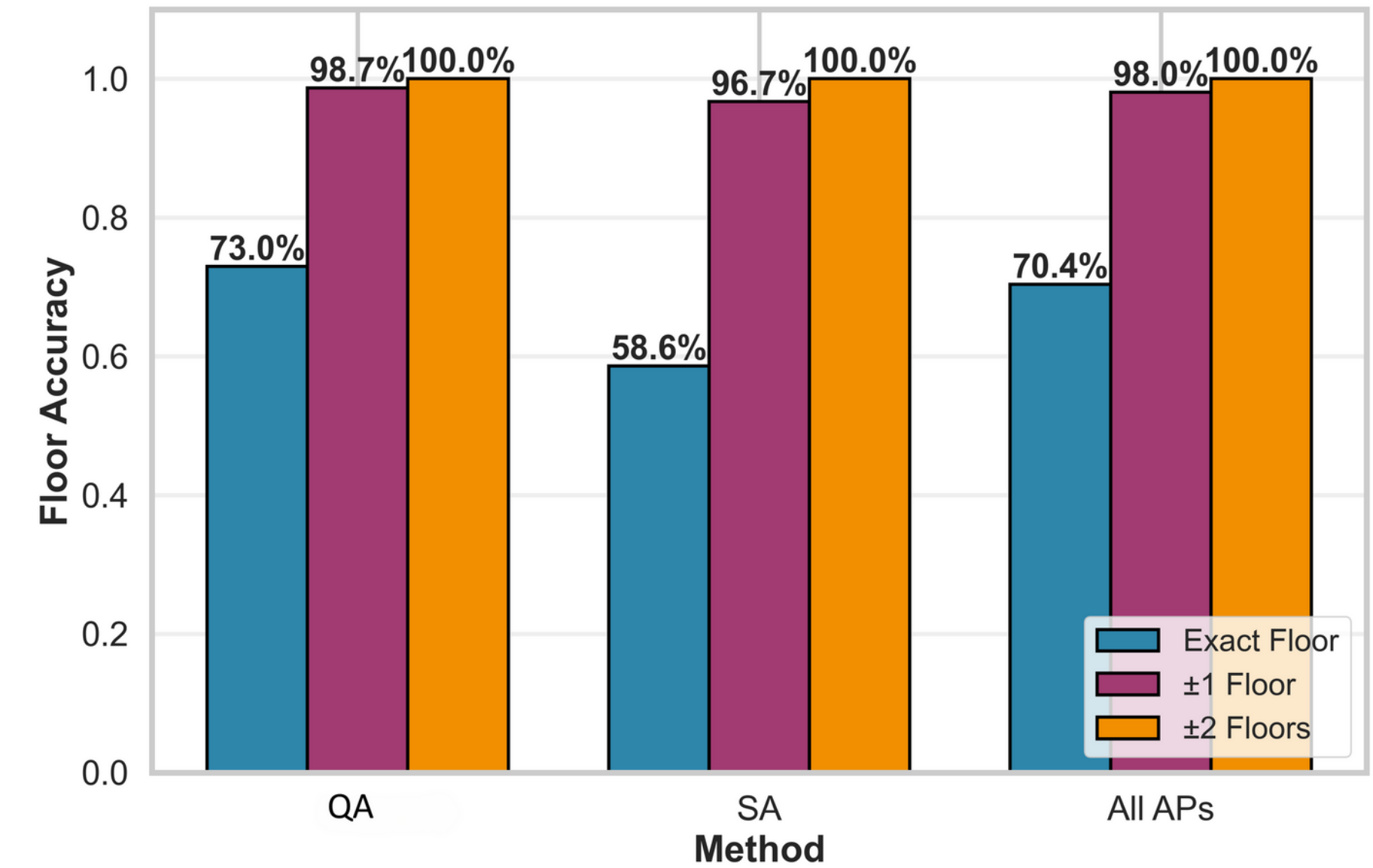


Fig. 11: Floor Accuracy across different Methods.

# 6.8 QA VS SA

- QA achieved the lowest localisation error
- QA is better than using all APs
- All APs have redundancy → decrease accuracy

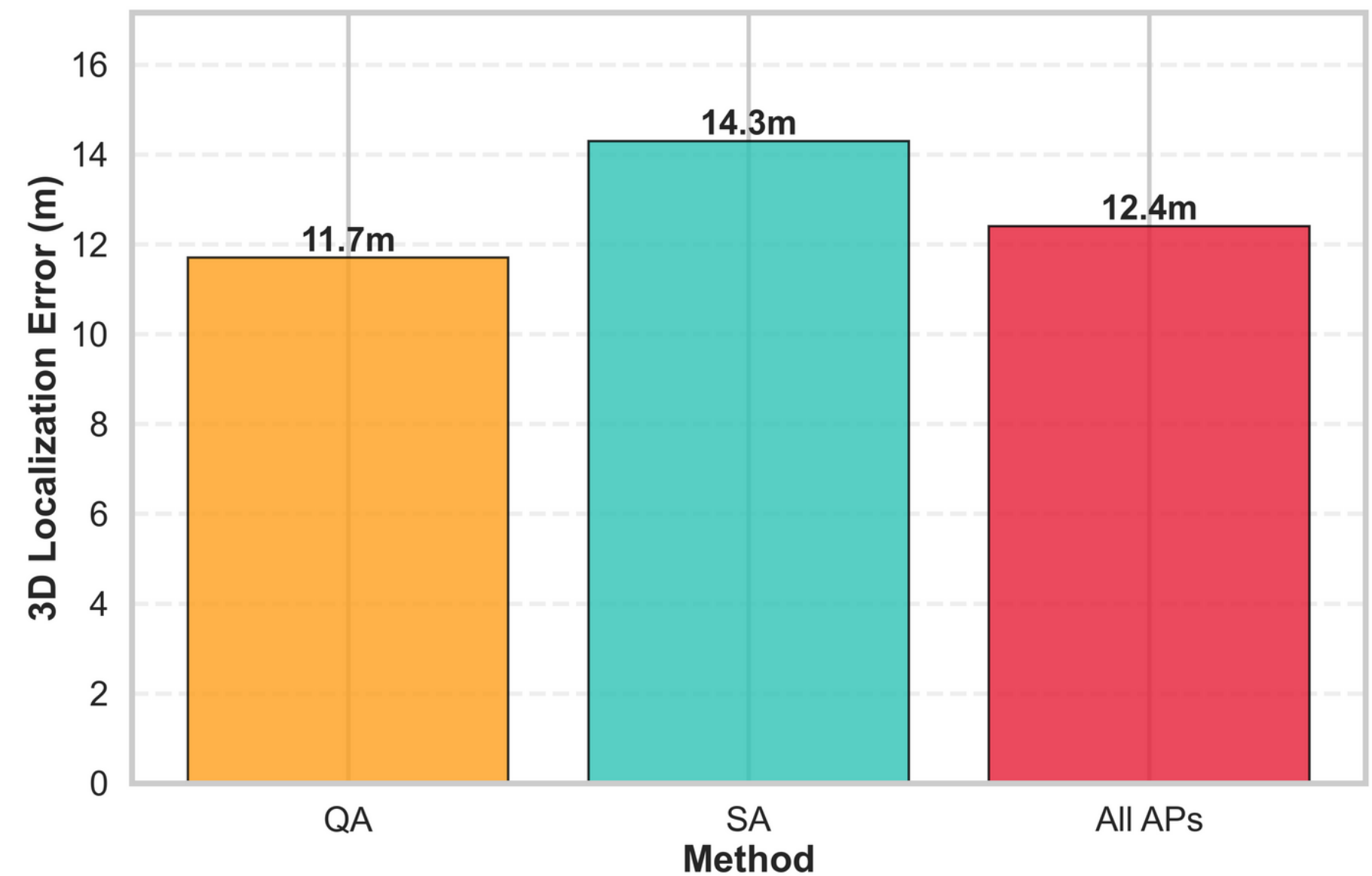


Fig. 12: Different Methods Impact on 3D Localization Accuracy.

# 6.8 QA VS SA

- Annealing time: duration over which the system is slowly evolved from an easy-to-prepare initial state to the final problem Hamiltonian.
- 61 Speed up the annealing time.

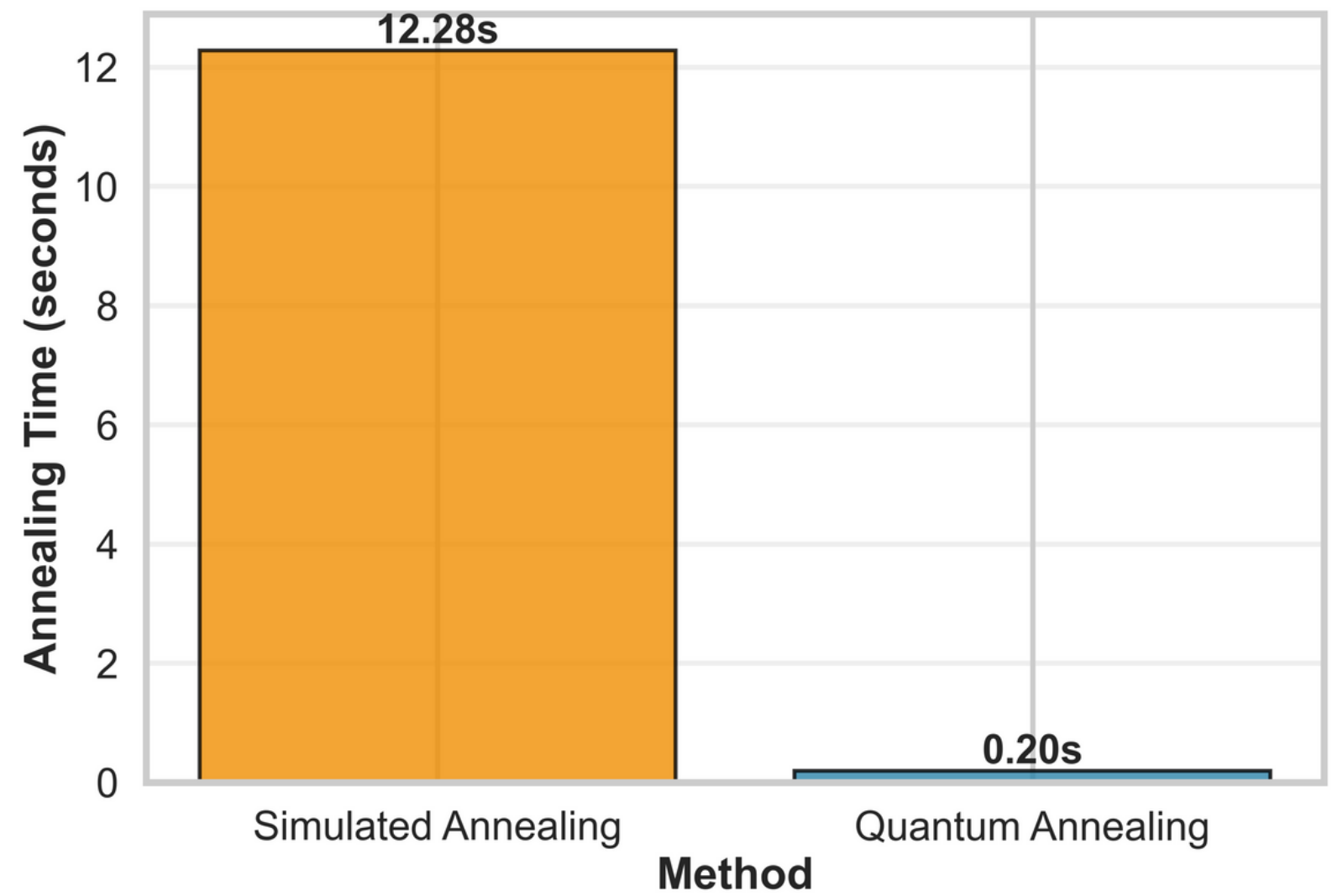


Fig. 13: Annealing time of SA VS QA.

# 7. Research Paper

## Quantum Optimization for Access Point Selection Under Budget Constraint

Anonymous Authors

**Abstract**—Optimal Access Point (AP) selection is crucial for accurate indoor localization, yet it is constrained by budget, creating a trade-off between localization accuracy and deployment cost. Classical approaches to AP selection are often computationally expensive, hindering their application in large-scale 3D indoor environments.

In this paper, we introduce a quantum APs selection algorithm under a budget constraint. The proposed algorithm leverages quantum annealing to identify the most effective subset of APs allowed within a given budget. We formulate the AP's selection problem as a quadratic unconstrained binary optimization (QUBO) problem, making it suitable for quantum annealing solvers. The proposed technique can drastically reduce infrastructure requirements with a negligible impact on performance.

We implement the proposed quantum algorithm and deploy it in a realistic 3D testbed. Our results demonstrate that this technique can drastically reduce infrastructure requirements, cutting the number of required APs by 96.1% with a negligible impact on performance. The proposed quantum approach outperforms classical AP selection algorithms in both accuracy and computational speed, achieving a solution in 0.20 seconds, a speedup of 61× over its classical counterpart, while reducing the mean localization error by 10% compared to the classical counterpart. For floor localization, the quantum approach achieves 73% floor accuracy, outperforming both the classical AP selection (58.6%) and even using the complete set of APs (70.4%). This highlights the promise of the proposed quantum AP selection algorithm for large-scale 3D localization systems.

**Index Terms**—Optimization, Quantum Computing, QUBO, Access Point selection, Indoor Localization

### I. INTRODUCTION

Indoor positioning systems have become increasingly critical for applications ranging from navigation assistance to asset tracking and emergency response [1]. While Global Positioning System (GPS) technology provides excellent outdoor localization accuracy, indoor environments present unique challenges including signal attenuation, multipath interference, and the absence of satellite connectivity [2]. Consequently, WiFi-based fingerprinting has emerged as the dominant approach for indoor localization, leveraging the ubiquity of wireless access points (APs) in modern buildings [3]–[6]. Leveraging Radio Frequency (RF) technology, WiFi-based fingerprinting systems function through a two-stage procedure. The initial offline phase involves constructing a radio map, or *RF fingerprint* by systematically collecting Received Signal Strength (RSS) data from transmitters such as WiFi access points, cell towers, and Bluetooth beacons at known locations across the site. Subsequently, in the online phase, the RSS readings from a device at an unknown location are gathered and matched against the pre-established fingerprint database to determine the most probable location based on signal similarity.

### II. BACKGROUND

#### A. Quantum Annealing

#### B. Fingerprinting in Indoor Localization

#### C. QUBO Objective

#### D. Importance

#### E. Methodology

#### F. Implementation and Evaluation

#### G. Conclusion

### III. METHODOLOGY

#### A. QUBO Objective

#### B. Importance

#### C. Methodology

#### D. Implementation and Evaluation

#### E. Conclusion

### IV. IMPLEMENTATION AND EVALUATION

#### A. Experimental Setup

#### B. Data Collection

#### C. Feature Extraction

#### D. Model Training

#### E. Model Testing

#### F. Results

#### G. Discussion

### V. CONCLUSION

#### A. Summary

#### B. Future Work

#### C. Acknowledgments

#### D. References

### VI. REFERENCES

#### A. Related Work

#### B. Proposed Approach

#### C. Evaluation

#### D. Limitations

#### E. Conclusion

### ACKNOWLEDGMENT

### REFERENCES

#### A. Related Work

#### B. Proposed Approach

#### C. Evaluation

#### D. Limitations

#### E. Conclusion

### ACKNOWLEDGMENT

### REFERENCES

#### A. Related Work

#### B. Proposed Approach

#### C. Evaluation

#### D. Limitations

#### E. Conclusion

### ACKNOWLEDGMENT

### REFERENCES

#### A. Related Work

#### B. Proposed Approach

#### C. Evaluation

#### D. Limitations

#### E. Conclusion

### ACKNOWLEDGMENT

### REFERENCES

#### A. Related Work

#### B. Proposed Approach

#### C. Evaluation

#### D. Limitations

#### E. Conclusion

### ACKNOWLEDGMENT

### REFERENCES

#### A. Related Work

#### B. Proposed Approach

#### C. Evaluation

#### D. Limitations

#### E. Conclusion

### ACKNOWLEDGMENT

### REFERENCES

#### A. Related Work

#### B. Proposed Approach

#### C. Evaluation

#### D. Limitations

#### E. Conclusion

### ACKNOWLEDGMENT

### REFERENCES

#### A. Related Work

#### B. Proposed Approach

#### C. Evaluation

#### D. Limitations

#### E. Conclusion

### ACKNOWLEDGMENT

### REFERENCES

#### A. Related Work

#### B. Proposed Approach

#### C. Evaluation

#### D. Limitations

#### E. Conclusion

### ACKNOWLEDGMENT

### REFERENCES

#### A. Related Work

#### B. Proposed Approach

#### C. Evaluation

#### D. Limitations

#### E. Conclusion

### ACKNOWLEDGMENT

### REFERENCES

#### A. Related Work

#### B. Proposed Approach

#### C. Evaluation

#### D. Limitations

#### E. Conclusion

### ACKNOWLEDGMENT

### REFERENCES

#### A. Related Work

#### B. Proposed Approach

#### C. Evaluation

#### D. Limitations

#### E. Conclusion

### ACKNOWLEDGMENT

### REFERENCES

#### A. Related Work

#### B. Proposed Approach

#### C. Evaluation

#### D. Limitations

#### E. Conclusion

### ACKNOWLEDGMENT

### REFERENCES

#### A. Related Work

#### B. Proposed Approach

#### C. Evaluation

#### D. Limitations

#### E. Conclusion

### ACKNOWLEDGMENT

### REFERENCES

#### A. Related Work

#### B. Proposed Approach

#### C. Evaluation

#### D. Limitations

#### E. Conclusion

### ACKNOWLEDGMENT

### REFERENCES

#### A. Related Work

#### B. Proposed Approach

#### C. Evaluation

#### D. Limitations

#### E. Conclusion

### ACKNOWLEDGMENT

### REFERENCES

#### A. Related Work

#### B. Proposed Approach

#### C. Evaluation

#### D. Limitations

#### E. Conclusion

### ACKNOWLEDGMENT

### REFERENCES

#### A. Related Work

#### B. Proposed Approach

#### C. Evaluation

#### D. Limitations

#### E. Conclusion

### ACKNOWLEDGMENT

### REFERENCES

#### A. Related Work

#### B. Proposed Approach

#### C. Evaluation

#### D. Limitations

#### E. Conclusion

### ACKNOWLEDGMENT

### REFERENCES

#### A. Related Work

#### B. Proposed Approach

# 7. Research Paper

2) **Variance-Based Importance:** The variance metric captures the spread of RSS measurements for each AP across all fingerprint locations:

$$I_i^{\text{VAR}} = \frac{1}{m-1} \sum_{l=1}^m (r_{i,l} - \bar{r}_i)^2 \quad (8)$$

where  $\bar{r}_i$  is the mean RSS for AP  $i$ . APs with high variance exhibit location-dependent signal characteristics, while low-variance APs provide little discriminative information.

3) **Average-Based Importance:** This metric uses the mean received signal strength as a proxy for AP  $i$  importance:

$$I_i^{\text{AVG}} = \bar{r}_i = \frac{1}{m} \sum_{l=1}^m r_{i,l} \quad (9)$$

This approach assumes that APs with stronger average signals are more reliable and contribute more to localization accuracy, though it ignores spatial variation patterns.

4) **Maximum-Based Importance:** This metric identifies APs based on their peak signal strength:

$$I_i^{\text{MAX}} = \max_{l=1,\dots,m} r_{i,l} \quad (10)$$

It assumes that APs with the highest maximum signal strength have better coverage and signal quality, potentially leading to more accurate localization.

## C. Redundancy

To quantify the pairwise redundancy between access points (APs), we compute a correlation matrix using the Pearson correlation coefficient applied to the received signal strength (RSS) data. Specifically, we consider only those APs with non-zero importance scores to ensure relevance. For each pair of relevant APs  $i$  and  $j$ , the absolute value of the Pearson correlation coefficient between their RSS vectors is calculated, producing a symmetric redundancy matrix  $R$  where each element  $R_{ij}$  represents the degree of redundancy between the corresponding APs. High values of  $R_{ij}$  indicate strong correlation and thus potential redundancy, which the selection algorithm aims to minimize to avoid overlapping or dependent information contributions.

$$R_{ij} = |\text{Corr}(r_i, r_j)| \quad (11)$$

$$= \left| \frac{\sum_{l=1}^m (r_{i,l} - \bar{r}_i)(r_{j,l} - \bar{r}_j)}{\sqrt{\sum_{l=1}^m (r_{i,l} - \bar{r}_i)^2} \sqrt{\sum_{l=1}^m (r_{j,l} - \bar{r}_j)^2}} \right| \quad (12)$$

## D. Budget Constraint

The parameter  $\alpha$  governs the trade-off between two objectives: maximizing the total importance of the selected access points and minimizing their mutual redundancy. The formulation ensures that both objectives are balanced for any given value of  $\alpha$ . However, tuning  $\alpha$  alone does not guarantee that exactly  $k$  APs will be selected. To enforce this budget constraint precisely, we introduce a penalty term  $\eta(\sum_{i=1}^n x_i - k)^2$ , where  $\eta$  is a sufficiently large weight that ensures the solution satisfies the requirement of selecting exactly  $k$  APs.

TABLE II: System parameters and their default values

Parameter	Default Value
AP Budget ( $k$ )	20
Importance-Redundancy Trade-off ( $\alpha$ )	0.8
Penalty Coefficient( $\eta$ )	2.0
Importance Metric	Entropy
Number of APs	1,000
Number of Sweeps	1,000
Inverse Temperature ( $\beta$ )	10.0
Transverse Field ( $\gamma$ )	1.0

## IV. EVALUATION

In this section, we evaluate our proposed quantum algorithm and implement it on a quantum machine simulator [42]. We start by describing our real testbed. Then, we show the effect of the different system parameters. Finally, we compare the proposed quantum algorithm with its classical counterpart. Table II shows our system parameters and their default values.

### A. Experiment Setup

The evaluation utilized a publicly available dataset covering a five-story building with a total area of approximately  $110\text{m}^2$  [43]. The dataset incorporates signals from 520 WiFi access points comprising both the building's own infrastructure and overhead APs from adjacent buildings. A fingerprinting database of  $m = 21,048$  samples was used for the experiments. Spatial coordinates (latitude, longitude) are normalized to  $[0,1]$ , while floor indices remain discrete integers. We set the floor height to 3.0 meters for 3D Euclidean distance calculations. For the floor classification task, a Random Forest Classifier was employed. All classical benchmarks were executed on a workstation equipped with a 12th Gen Intel Core i7-12700H processor running at 2.30 GHz with 16 GB RAM, operating on Windows 11 (64-bit).

For solving the QUBO formulation, we employ OpenJij [42] which is an open-source framework for quantum annealing simulation that implements quantum Monte Carlo methods. The quantum annealing parameters are set to 1,000 reads (independent optimization runs) and 1,000 sweeps (Monte Carlo steps per run), ensuring sufficient exploration of the solution space. In the next subsections, we perform comprehensive hyperparameter optimization across QUBO parameters ( $k, \alpha, \eta$ ) and annealing-specific parameters (num\_sweeps, inverse temperature  $\beta$ ) to identify optimal configurations. Performance is evaluated using 3D localization error, floor classification accuracy, and time-to-solution (TTS) metrics, with all results representing mean and standard deviation over multiple independent trials. As a comparison baseline, we utilize Simulated Annealing (SA) sampler [44], which implements classical simulated annealing without quantum tunneling effects.

### B. Importance

Figure 2 compares the performance of the proposed four importance metrics for AP selection. The figure shows that entropy-based importance achieves the best mean 3D localization error of 11.58m, demonstrating that signal variability

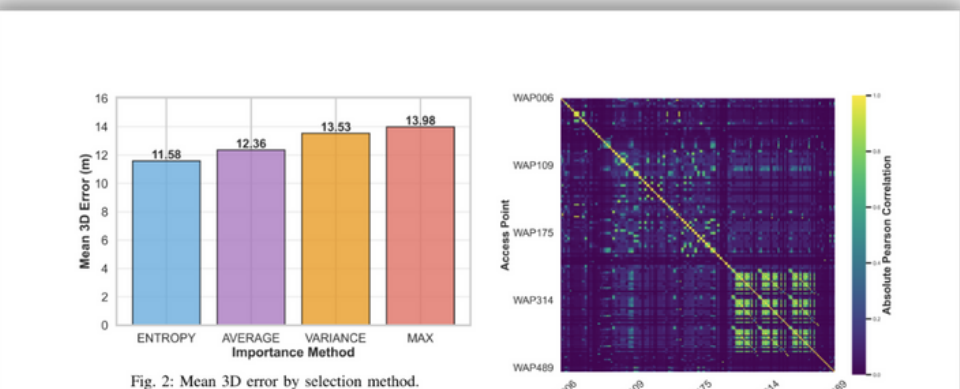


Fig. 2: Mean 3D error by selection method.

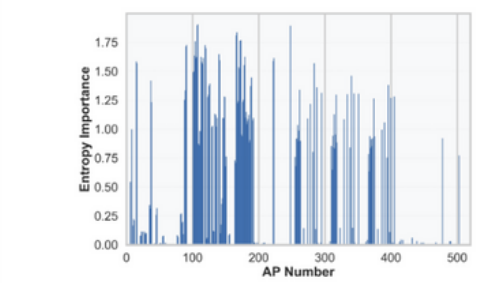


Fig. 3: Entropy Importance.

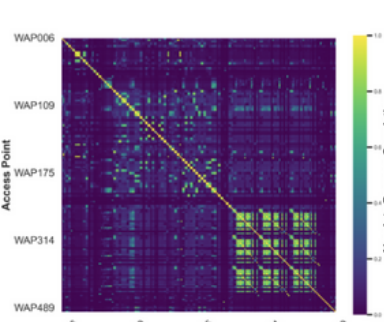


Fig. 4: Pairwise correlation matrix of AP RSS patterns.

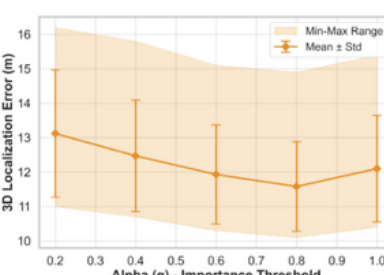


Fig. 5: Effect of  $\alpha$  parameter on mean 3D localization error.

measured through Shannon entropy most effectively identifies informative APs. This result indicates that for fingerprinting-based localization, consistent signal patterns across diverse locations are more valuable than peak signal strength or high variability alone. Figure 3 further shows the Entropy importance score computed for every access point in the environment. The distribution reveals that a substantial number of APs contribute very little to the localization model. Pruning these low-importance APs can significantly reduce the system's computational complexity while having a negligible impact on localization accuracy.

### C. Redundancy

Figure 4 visualizes the correlation matrix for the access points, revealing significant redundancy among numerous AP pairs (indicated by the yellow regions). This correlation introduces extra computational overhead without yielding a corresponding improvement in localization accuracy.

### D. Effect of QUBO Parameters

#### 1) Effect of Balancing Parameter $\alpha$ :

Figure 5 illustrates the effect of the  $\alpha$  parameter on 3D localization accuracy, where

the  $\alpha$  controls the trade-off between importance maximization and redundancy minimization in the QUBO objective. The figure suggests that heavily weighting importance (e.g., at  $\alpha = 0.80$ ) produces consistent average results, which demonstrates that the QUBO formulation effectively balances both the importance and redundancy.

#### 2) Effect of Penalty Parameter $\eta$ :

Figure 6 shows the effect of increasing the penalty parameter  $\eta$  on the selected number of APs (at budget  $k = 20$ ). Figure 7 further shows the 3D localization accuracy.

The figures show that, for small values of the penalty, the optimizer can reach the target of  $k$  APs, with a minimum localization accuracy at  $\eta = 2$ . For larger penalty values, the constraint term creates an overly harsh energy landscape, causing the annealer to get trapped in local minima before reaching the target number of APs  $k$ , which in turn affects the localization accuracy.

#### 3) Effect of The Budget Parameter $k$ :

Figure 8 illustrates the relationship between the AP budget  $k$  and the resulting

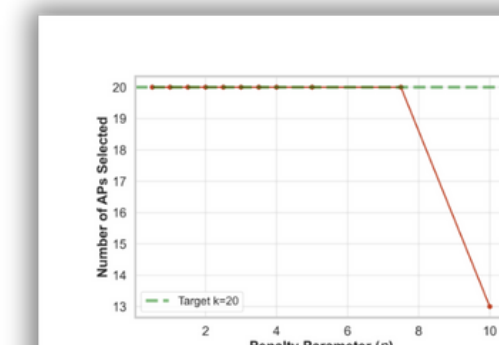


Fig. 6:  $\eta$  Impact on the Number of Selected APs.

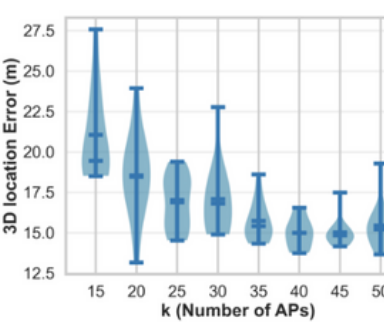


Fig. 7:  $\eta$  Impact on the 3D Mean Error.

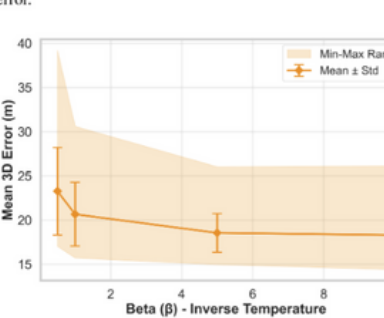


Fig. 8: Effect of increasing budget  $k$  on the 3D localization error.

problem with a high probability, encompassing annealing time, the number of iterations, and all associated overhead. As expected, the results show that a higher number of sweeps directly leads to an increased TTS. This relationship is intuitive because each sweep represents a fundamental update step in the annealing process. In this context,  $\beta$  functions as a scaling factor that controls the influence of the problem's energy landscape, effectively determining how sharply the solver distinguishes between optimal and suboptimal solutions. The figure shows that localization accuracy improves as  $\beta$  increases because a higher value helps the annealer to more effectively navigate the complex cost function and settle into a deeper, more optimal energy state corresponding to a better AP selection. However, this improvement saturates beyond a value of  $\beta = 5$ .

2) **Effect of Inverse Temperature Parameter  $\beta$ :** Figure 9 demonstrates the impact of the inverse temperature parameter  $\beta$  on 3D localization accuracy in the quantum annealing process. In this context,  $\beta$  functions as a scaling factor that controls the influence of the problem's energy landscape, effectively determining how sharply the solver distinguishes between optimal and suboptimal solutions. The figure shows that localization accuracy improves as  $\beta$  increases because a higher value helps the annealer to more effectively navigate the complex cost function and settle into a deeper, more optimal energy state corresponding to a better AP selection. However, this improvement saturates beyond a value of  $\beta = 5$ .

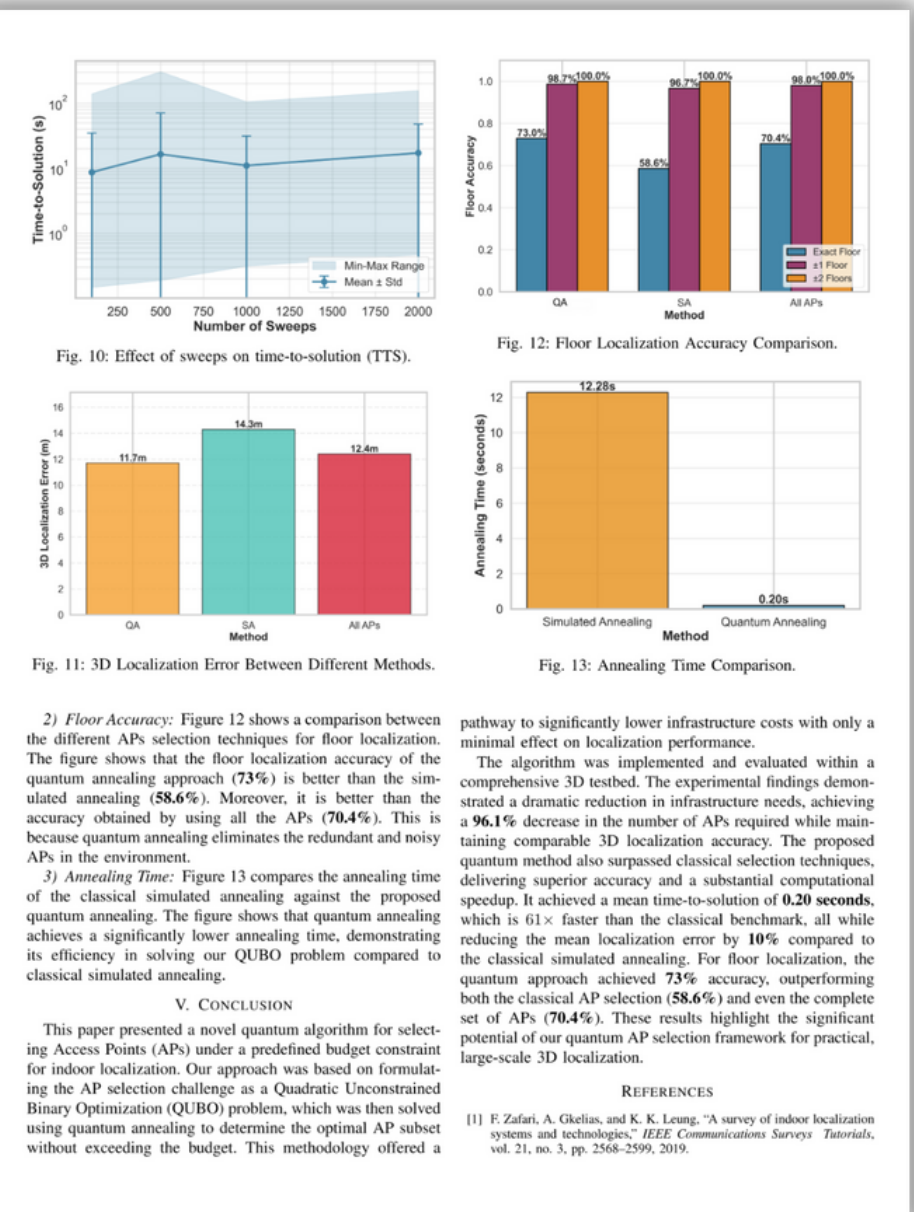
3) **Number of Sweeps:** Figure 10 illustrates the effect of the number of sweeps on the time-to-solution (TTS). TTS represents the total time required to successfully solve the

problem with a high probability, encompassing annealing time, the number of iterations, and all associated overhead.

As expected, the results show that a higher number of sweeps directly leads to an increased TTS. This relationship is intuitive because each sweep represents a fundamental update step in the annealing process. In this context,  $\beta$  functions as a scaling factor that controls the influence of the problem's energy landscape, effectively determining how sharply the solver distinguishes between optimal and suboptimal solutions. The figure shows that localization accuracy improves as  $\beta$  increases because a higher value helps the annealer to more effectively navigate the complex cost function and settle into a deeper, more optimal energy state corresponding to a better AP selection. However, this improvement saturates beyond a value of  $\beta = 5$ .

4) **Comparison with Classical APs Selection:** Figure 11 presents the mean 3D localization error across the different AP selection methods. The figure shows that the quantum annealing approach (QA) achieves a mean error of **11.7m**, which is lower than simulated annealing (SA) at **14.3m** and lower than using all APs having error of **12.4m**. This demonstrates that our quantum AP selection selects a more effective subset than classical optimization methods, identifying truly informative APs while eliminating redundancy.

# 7. Research Paper



**2) Floor Accuracy:** Figure 12 shows a comparison between the different APs selection techniques for floor localization. The figure shows that the floor localization accuracy of the quantum annealing approach (73%) is better than the simulated annealing (58.6%). Moreover, it is better than the accuracy obtained by using all the APs (70.4%). This is because quantum annealing eliminates the redundant and noisy APs in the environment.

**3) Annealing Time:** Figure 13 compares the annealing time of the classical simulated annealing against the proposed quantum annealing. The figure shows that quantum annealing achieves a significantly lower annealing time, demonstrating its efficiency in solving our QUBO problem compared to classical simulated annealing.

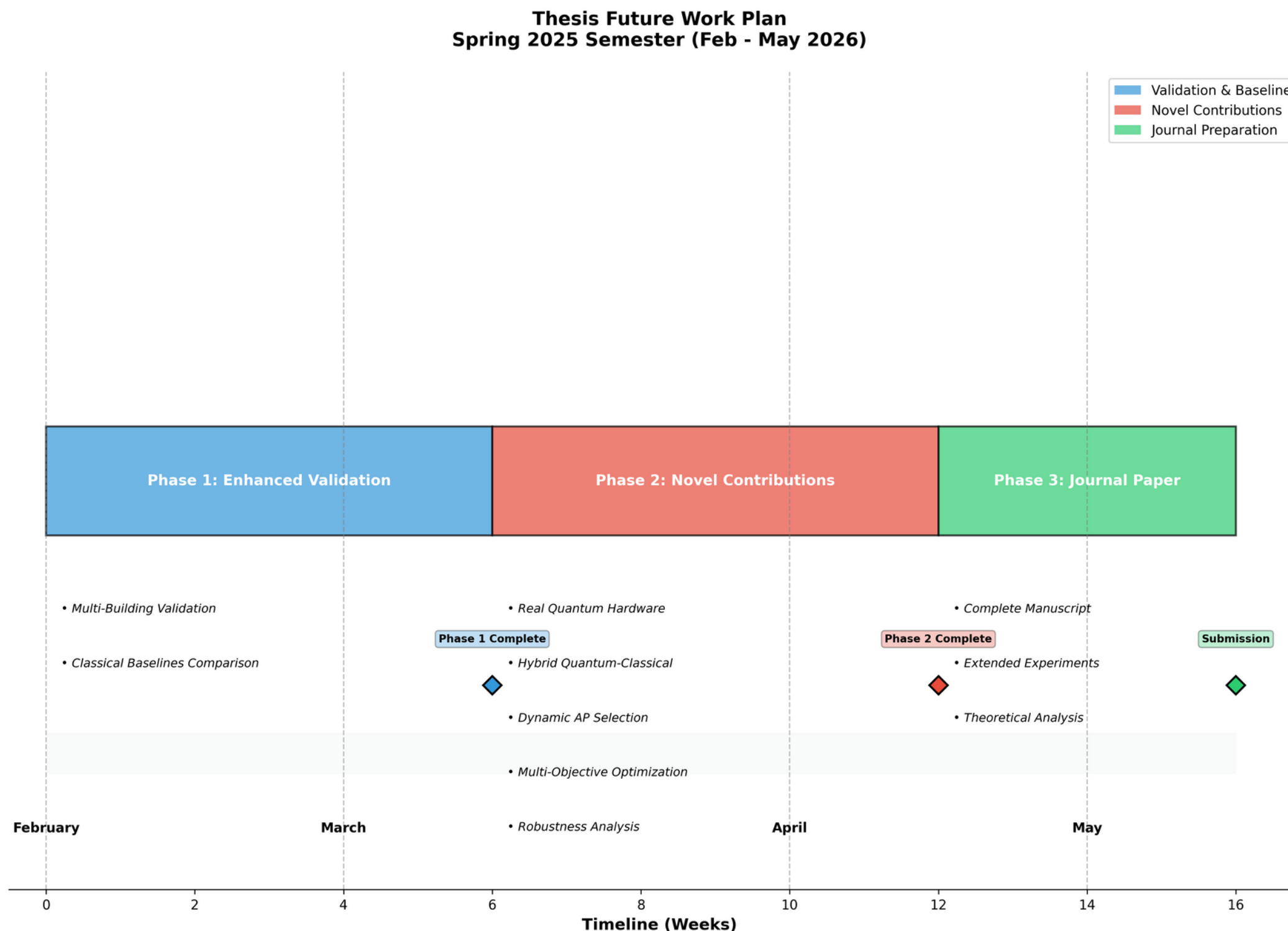
## V. CONCLUSION

This paper presented a novel quantum algorithm for selecting Access Points (APs) under a predefined budget constraint for indoor localization. Our approach was based on formulating the AP selection challenge as a Quadratic Unconstrained Binary Optimization (QUBO) problem, which was then solved using quantum annealing to determine the optimal AP subset without exceeding the budget. This methodology offered a

## REFERENCES

- [1] F. Zafari, A. Gkelias, and K. K. Leung, "A survey of indoor localization systems and technologies," *IEEE Communications Surveys Tutorials*, vol. 21, no. 3, pp. 2568–2599, 2019.
- [2] H. Liu, H. Darabi, P. Banerjee, and J. Liu, "Survey of wireless indoor positioning techniques and systems," *IEEE Transactions on Systems, Man, and Cybernetics, Part C (Applications and Reviews)*, vol. 37, no. 6, pp. 1067–1080, 2007.
- [3] P. Balaji and V. N. Padmanabhan, "Radar: An in-building rf-based user location and tracking system," in *Proceedings IEEE INFOCOM 2000. Conference on computer communications. Nineteenth annual joint conference of the IEEE computer and communications societies (Cat. No. 00CH37064)*, vol. 2. Ieee, 2000, pp. 775–784.
- [4] M. Yousefi and A. Agrawala, "The hornbeam location determination system," in *Proceedings of the 3rd international conference on Mobile systems, applications, and services*, 2005, pp. 205–218.
- [5] S. He and S.-H. G. Chan, "Wi-fi fingerprint-based indoor positioning: Recent advances and comparisons," *IEEE Communications Surveys & Tutorials*, vol. 18, no. 1, pp. 466–490, 2016.
- [6] G. Deak, K. Curran, and J. Connell, "A survey of active and passive indoor localisation systems," *Computer Communications*, vol. 35, no. 16, pp. 1939–1954, 2012. [Online]. Available: <https://www.sciencedirect.com/science/article/pii/S014036641200196X>
- [7] S. Xia, Y. Liu, G. Yuan, M. Zhu, and Z. Wang, "Indoor fingerprint positioning based on wi-fi: An overview," *ISPRS International Journal of Geo-Information*, vol. 6, no. 5, p. 135, 2017.
- [8] R. Elbakly, H. Aly, and M. Youssef, "Trusted: Accurate and robust rf-based floor estimation for challenging indoor environments," *IEEE Sensors Journal*, vol. 18, no. 24, pp. 10115–10124, 2018.
- [9] X. Guo, N. Ansari, F. Hu, Y. Shao, N. R. Elikplim, and L. Li, "A survey on 3d indoor localization systems," *IEEE Communications Surveys & Tutorials*, vol. 19, no. 3, pp. 1917–1950, 2017.
- [10] J. Luo, L. Fan, and H. Li, "Indoor positioning systems based on visible light communication: State of the art," *IEEE Communications Surveys & Tutorials*, vol. 19, no. 24, pp. 10115–10124, 2017.
- [11] S. He and S.-H. G. Chan, "Efficient access point selection for indoor localization with wi-fi fingerprint," *IEEE Wireless Communications Letters*, vol. 4, no. 1, pp. 49–52, 2015.
- [12] K. Kaemarungsi and P. Krishnamurthy, "Distribution of wlan received signal strength indication for indoor location determination," in *Proceedings of the 1st IEEE International Symposium on Wireless Pervasive Computing*. IEEE, 2004, pp. 6–10.
- [13] W. Li, D. Wei, H. Yuan, and G. Ouyang, "Access point selection for wlan indoor positioning based on spatial information," *International Journal of Distributed Sensor Networks*, vol. 11, no. 5, p. 841978, 2015.
- [14] C. Zhou and A. Wieser, "Faccard analysis and lasso-based feature selection for location fingerprinting with limited computational complexity," in *LBS 2018: 14th International Conference on Location Based Services*. Springer, Cham, 2018, pp. 71–87, extended version available as arXiv:1711.07812.
- [15] J.-R. Jiang, H. Subakti, and H.-S. Liang, "Fingerprint feature extraction for indoor localization," *Sensors*, vol. 21, no. 16, p. 5434, 2021. [Online]. Available: <https://doi.org/10.3390/s21165434>
- [16] P. Costa, G. D'Souza, P. Silva, and P. Portugal, "A mutual information based online access point selection strategy for wifi indoor localization," in *2015 IEEE International Conference on Automation Science and Engineering (CASE)*. IEEE, 2015, pp. 180–185. [Online]. Available: <https://doi.org/10.1109/CoASE.2015.7294059>
- [17] A. Shokry and M. Youssef, "A deployable quantum access points selection algorithm for large-scale localization," *arXiv preprint arXiv:2407.08943*, 2024. [Online]. Available: <https://arxiv.org/abs/2407.08943>
- [18] C. C. McGeoch, "Adiabatic quantum computation and quantum annealing: Theory and practice," *Synthesis Lectures on Quantum Computing*, vol. 5, no. 2, pp. 1–93, 2014.
- [19] T. Kadokawa and H. Nishimori, "Quantum annealing in the transverse ising model," *Physical Review E*, vol. 58, no. 5, pp. 5355–5363, 1998.
- [20] E. Farhi, J. Goldstone, S. Gutmann, and M. Sipser, "Quantum computation by adiabatic evolution," *arXiv preprint quant-ph/0001106*, 2000, available at <https://arxiv.org/abs/quant-ph/0001106>.
- [21] T. Albash and D. A. Lidar, "Adiabatic quantum computation," *Reviews of Modern Physics*, vol. 90, no. 1, p. 015002, 2018.
- [22] D. Aharonov, W. Van Dam, J. Kempe, Z. Landau, S. Lloyd, and O. Regev, "Adiabatic quantum computation is equivalent to standard quantum computation," *SIAM Review*, vol. 50, no. 4, pp. 755–787, 2008.
- [23] M. W. Johnson, M. H. S. Amin, S. Gildert, T. Lanting, F. Hamze, N. Dickson, R. Harris, A. J. Berkley, J. Johansson, P. Bunyk et al., "Quantum annealing with manufactured spins," *Nature*, vol. 473, no. 7346, pp. 194–198, 2011.
- [24] S. Mukundan, T. Albash, and D. A. Lidar, "Tunneling and speedup in quantum optimization for permutation-symmetric problems," *Physical Review X*, vol. 6, no. 3, p. 031010, 2016.
- [25] D. J. Griffiths and D. F. Schroeter, *Introduction to Quantum Mechanics*. Cambridge, UK: Cambridge University Press, 2018.
- [26] G. E. Santoro, R. Martonak, E. Tosatti, and R. Car, "Theory of quantum annealing of an Ising spin glass," *Science*, vol. 295, no. 5564, pp. 2427–2430, 2002.
- [27] A. Lucas, "Ising formulations of many NP problems," *Frontiers in Physics*, vol. 2, p. 5, 2014.
- [28] G. Kochenberger, J.-K. Hao, F. Glover, M. Lewis, Z. Lü, H. Wang, and Y. Wang, "The unconstrained binary quadratic programming problem: A survey," *Journal of Combinatorial Optimization*, vol. 28, no. 1, pp. 58–81, 2014.
- [29] F. Glover, G. Kochenberger, R. Hennig, and Y. Du, "Quantum bridge analytics i: a tutorial on formulating and using qubo models," *Annals of Operations Research*, vol. 314, no. 1, pp. 141–183, 2022. [Online]. Available: <https://doi.org/10.1007/s10479-022-04634-2>
- [30] E. Boros and P. L. Hammer, "Pseudo-boolean optimization," *Discrete Applied Mathematics*, vol. 123, no. 1–3, pp. 155–225, 2002.
- [31] S. G. Brush, "History of the Ising-Ising model," *Reviews of Modern Physics*, vol. 39, no. 4, pp. 883–893, 1967.
- [32] F. Barahona, "On the computational complexity of Ising spin glass models," *Journal of Physics A: Mathematical and General*, vol. 15, no. 10, pp. 3241–3253, 1982.
- [33] V. Choi, "Minor-embedding in adiabatic quantum computation: I. the parameter setting problem," *Quantum Information Processing*, vol. 7, no. 5, pp. 193–209, 2008.
- [34] S. Boixo, T. F. Ronnow, S. V. Isakov, Z. Wang, D. Wecker, D. A. Lidar, J. M. Martinis, and M. Troyer, "Evidence for quantum annealing with more than one hundred qubits," *Nature Physics*, vol. 10, no. 3, pp. 218–224, 2014.
- [35] D-Wave Systems, "D-wave advantage system: Technology overview," <http://www.dwavesys.com>, 2020, white paper.
- [36] R. Ober, S. Muggenthaler, and E. Schuster, "Quantum computing for finance: Overview and prospects," *Reviews in Physics*, vol. 4, p. 100028, 2019.
- [37] F. Neukart, G. Compagno, C. Seidel, D. von Dollen, S. Yarkoni, and B. Parney, "Traffic flow optimization using a quantum annealer," *Frontiers in ICT*, vol. 4, p. 29, 2017.
- [38] R. Nath, H. Thapliyal, and T. S. Humble, "A review of machine learning classification using quantum annealing for real-world applications," *SN Computer Science*, vol. 2, no. 6, p. 428, 2021.
- [39] D. Venturelli, S. Mandrà, S. Knysh, B. O’Gorman, R. Biswas, and V. Smelyanskiy, "Quantum optimization of fully connected spin glasses," *Physical Review X*, vol. 5, no. 3, p. 031040, 2015.
- [40] S. Shang, S. Shen, L. Song, J. Xie, J. Chen, and Z. Song, "Overview of wifi fingerprinting-based indoor positioning," *IET Communications*, vol. 16, no. 7, pp. 753–765, 2022.
- [41] R. M. Safwat, H. El-Fakharami, N. El-Bendary, and A. E. Hassanien, "Fingerprinting based indoor localization using deep CNN," *International Journal of Intelligent Computing and Information Sciences*, vol. 23, no. 2, pp. 143–154, 2023.
- [42] J. Inc., "OpenJij: Open-source framework for optimization and sampling on the Ising model," 2022, documentation: <https://tutorial.openjij.org>. [Online]. Available: <https://github.com/OpenJij/OpenJij>
- [43] J. Torres-Sospedra, R. Montolí, A. Martínez-Usó, J. P. Avariento, T. J. Arnau, M. Benedí, D. Bordonau, and J. Huerta, "Ujindoofloc: A new multi-building and multi-floor database for wlan fingerprint-based indoor localization problems," in *2014 International Conference on Indoor Positioning and Indoor Navigation (IPIN)*. IEEE, 2014, pp. 261–270.
- [44] D-Wave Systems Inc., "dwave-neal: Simulated Annealing Sampler," 2022, version 0.5.9. [Online]. Available: <https://github.com/dwavesystems/dwave-neal>

# 8. Future Work





# THANK YOU

Any Questions?



# Appendix: Key Terms & Acronyms

## AP (Access Point)

- WiFi router or transmitter that broadcasts wireless signals
- Used as reference points for indoor localization

## RSS (Received Signal Strength)

- Power level of WiFi signal received at a device
- Measured in dBm (decibel-milliwatts)
- Typically ranges from -30 dBm (strong) to -90 dBm (weak)

## QUBO (Quadratic Unconstrained Binary Optimization)

- Optimization problem with binary variables (0 or 1)
- Objective function contains quadratic and linear terms
- Native format for quantum annealers

## 3D Localization

- Determining position in three-dimensional space
- Includes latitude (x), longitude (y), and floor/altitude (z)

## Fingerprinting

- Indoor positioning technique using signal patterns
- Creates "fingerprint" of signal characteristics at each location
- Matches new measurements to database

## Quantum Annealing

- Optimization technique using quantum mechanics
- Exploits superposition and tunneling
- Specialized for combinatorial optimization problems

## Hamiltonian

- Mathematical operator representing total energy of quantum system
- $H(t) = (1-s(t))H_0 + s(t)H_f$
- Evolution from simple  $H_0$  to problem-encoding  $H_f$

## Quantum Tunneling

- Quantum phenomenon allowing particles to pass through energy barriers
- Enables escape from local minima
- Key advantage over classical optimization

## Adiabatic Evolution

- Slow transformation of quantum state
- System remains in ground state if evolution is slow enough
- Foundation of quantum annealing

## Ising Model

- Model of interacting atomic spins
- Equivalent representation of QUBO problems
- Native format for quantum hardware